JOURNAL OF BACTERIOLOGY, Apr. 2010, p. 1774–1784 Vol. 192, No. 7
0021-9193/10/$12.00 doi:10.1128/JB.01132-09

Pyruvate Carboxylase Plays a Crucial Role in Carbon Metabolism of Extra- and Intracellularly Replicating *Listeria monocytogenes*▽

Jennifer Schär,[1]†§ Regina Stoll,[1]† Kristina Schauer,[2] Daniela I. M. Loeffler,[1]‡ Eva Eylert,[3] Biju Joseph,[4] Wolfgang Eisenreich,[3] Thilo M. Fuchs,[2]* and Werner Goebel[5]

Lehrstuhl für Mikrobiologie, Biozentrum, Universität Würzburg, D-97074 Würzburg, Germany[1]; Zentralinstitut für Ernährungs- und Lebensmittelforschung, Abteilung Mikrobiologie, Technische Universität München, D-85350 Freising, Germany[2]; Lehrstuhl für Biochemie, Technische Universität München, D-85747 Garching, Germany[3]; Institut für Hygiene und Mikrobiologie, Universität Würzburg, D-97080 Würzburg, Germany[4]; and Max von Pettenkofer-Institut für Hygiene und Medizinische Mikrobiologie, Ludwig-Maximilians-Universität, D-80336 Munich, Germany[5]

Received 25 August 2009/Accepted 23 December 2009

The human pathogen *L. monocytogenes* is a facultatively intracellular bacterium that survives and replicates in the cytosol of many mammalian cells. The listerial metabolism, especially under intracellular conditions, is still poorly understood. Recent studies analyzed the carbon metabolism of *L. monocytogenes* by the ^{13}C isotopologue perturbation method in a defined minimal medium containing [U-$^{13}C_6$]glucose. It was shown that these bacteria produce oxaloacetate mainly by carboxylation of pyruvate due to an incomplete tricarboxylic acid cycle. Here, we report that a *pycA* insertion mutant defective in pyruvate carboxylase (PYC) still grows, albeit at a reduced rate, in brain heart infusion (BHI) medium but is unable to multiply in a defined minimal medium with glucose or glycerol as a carbon source. Aspartate and glutamate of the *pycA* mutant, in contrast to the wild-type strain, remain unlabeled when [U-$^{13}C_6$]glucose is added to BHI, indicating that the PYC-catalyzed carboxylation of pyruvate is the predominant reaction leading to oxaloacetate in *L. monocytogenes*. The *pycA* mutant is also unable to replicate in mammalian cells and exhibits high virulence attenuation in the mouse sepsis model.

Listeria monocytogenes is a human pathogen that can cause systemic infections, especially in immunocompromised people, with symptoms such as septicemia, (encephalo)meningitis, placentitis, and stillbirth. These Gram-positive bacteria are able to enter the cytosol of many mammalian cells after being taken up via normal or induced phagocytosis by professional phagocytes, mainly macrophages and dendritic cells, and nonphagocytic cells, such as epithelial cells, fibroblasts, and endothelial cells (1, 8, 13). While the virulence genes and their regulation (4, 21), as well as the encoded virulence factors (20, 22), necessary for the various steps of the intracellular replication cycle of *L. monocytogenes* have been extensively studied in the past few decades, there is still little information concerning the metabolic capacities and the metabolic adaptation processes (10) that enable these bacteria to efficiently replicate in the cytosol of their host cells.

The information on listerial metabolism obtained from the genome sequence (7) suggests that these heterotrophic bacteria are capable of utilizing a variety of carbohydrates as carbon sources, since a large number of genes encoding phosphoenolpyruvate (PEP)-phosphotransferase systems (PTS) were identified. Furthermore, all genes encoding the enzymes necessary for the catabolism of glycerol and dihydroxyacetone are present in the *L. monocytogenes* genome (7, 11). This genomic information is in accord with data from previous and more recent physiological studies (11, 17, 24).

Most genes encoding the enzymes for the major catabolic pathways, namely, glycolysis, the citrate cycle, and the pentose phosphate cycle, are present in *L. monocytogenes*. The citrate cycle, however, seems to be interrupted, since the genes encoding 2-oxoglutarate dehydrogenase have not been identified in all *L. monocytogenes* strains sequenced so far, including EGD-e (7), or in *Listeria innocua* strain Clip 11262. This enzymatic gap in the citrate cycle was recently confirmed by ^{13}C isotopologue perturbation studies using uniformly ^{13}C-labeled glucose. The results showed that two C_4 amino acids, aspartate and threonine, are generated in *L. monocytogenes*, predominantly from building blocks comprising one or three ^{13}C atoms, respectively (2). These data suggested that oxaloacetate, the direct or indirect precursor of both amino acids, is generated by an anaplerotic reaction assembling precursors composed of one and three carbon atoms, respectively. This can be afforded by the carboxylation of pyruvate catalyzed by the ATP-dependent pyruvate carboxylase (PYC) encoded by *pycA*.

The genes encoding the enzymes for most anabolic pathways, but not those for the biosynthesis of thiamine (vitamin B_1), riboflavin (vitamin B_2), biotin, and thiotic acid (lipoate), were also identified in *L. monocytogenes*. However, these bacteria grow efficiently in a mineral salt medium containing a suitable carbon source (e.g., glucose) and these four cofactors

* Corresponding author. Mailing address: Zentralinstitut für Ernährungs- und Lebensmittelforschung (ZIEL), Abteilung Mikrobiologie, Technische Universität München, Weihenstephaner Berg 3, D-85354 Freising, Germany. Phone: 49-8161-713859. Fax: 49-8161-714492. E-mail: thilo.fuchs@wzw.tum.de.

† J.S. and R.S. contributed equally to this work.

§ Present address: Tierärztliche Fakultät, Lehrstuhl für Tierzucht und Allgemeine Landwirtschaftslehre, Ludwig-Maximilians-Universität, D-80539 Munich, Germany.

‡ Present address: Department of Paediatrics, Division of Infectious and Immunological Diseases, Child and Family Research Institute, UBC, Vancouver, BC, Canada.

▽ Published ahead of print on 22 January 2010.

only when the amino acids cysteine, methionine, glutamine, arginine, valine, isoleucine, and leucine are also added (17). According to Tsai and Hodgson, strain 10403S requires only methionine and cysteine (24). The missing sulfate reductase in *L. monocytogenes* readily explains the strict requirement for cysteine/methionine as a sulfur source, while the missing nitrate reductase may be the reason for the stimulatory growth effect of glutamine and arginine as reduced nitrogen sources. However, the need for the three branched-chain amino acids (BCAA) valine, isoleucine, and leucine for efficient growth of *L. monocytogenes* EGD-e (references 17 and 24 and our unpublished results) is less obvious, since *L. monocytogenes* has the complete genetic set for synthesis of the BCAA, indicating the role of metabolic intermediates in listerial growth.

The central precursor for the biosynthesis of the BCAA is pyruvate, which is channeled into their biosynthetic pathways either directly, via oxidative decarboxylation of pyruvate to acetyl-coenzyme A (CoA), or more indirectly via oxaloacetate (generated by pyruvate carboxylation) to aspartate and further to threonine. Thus, biosynthesis of the BCAA may compete with the PYC-mediated generation of oxaloacetate for the common substrate pyruvate. These data suggest that PYC may play an important role in the carbon metabolism of *L. monocytogenes*.

To more precisely determine the significance of this anaplerotic enzyme for listerial metabolism and pathogenesis, we generated a mutant of *L. monocytogenes* EGD-e defective in *pycA*, the gene encoding PYC, and studied the replication of this mutant under different extra- and intracellular growth conditions. The results show that PYC indeed plays a crucial role in the intracellular replication of *L. monocytogenes* and hence in the infection process.

MATERIALS AND METHODS

Bacterial strains and growth conditions. The *Escherichia coli* strain DH5α was used for cloning, and pLSV101 was used as a construction vector for mutagenesis (16). *E. coli* strains were cultivated in Luria-Bertani (LB) medium at 37°C. The *L. monocytogenes* wild-type strain EGD-e and the mutant strains were grown under aerobic conditions in brain heart infusion (BHI) or in chemically defined minimal medium (MM) (17) supplemented with different sugars or other carbon sources at 37°C or 42°C. When necessary, the media were supplemented with erythromycin (Sigma, St. Louis, MO) to final concentrations of 5 μg/ml for *L. monocytogenes* or 300 μg/ml for *E. coli*. Fresh stock solutions of carbohydrates (glucose or glycerol) or other supplements (adenosine, oxaloacetate, or Casamino Acids [CAA]) were filter sterilized and added to the culture medium at the required final concentrations. To determine growth curves, aliquots were removed at regular intervals, and the optical density (OD) was determined using a spectrophotometer. For shift experiments, overnight cultures of the strains were diluted in fresh BHI, grown to an OD at 600 nm (OD_{600}) of 0.5, and washed once in sterile phosphate-buffered saline (PBS). The sedimented cells were resuspended in MM containing the appropriate supplement(s), and growth was subsequently monitored at 37°C.

For mouse infection experiments, *L. monocytogenes* strains were grown to the mid-logarithmic phase (OD_{600} = 1.0) at 37°C in BHI medium, washed two times with endotoxin-free isotonic saline (0.9% NaCl), resuspended in 20% (vol/vol) glycerol in 0.9% NaCl, and stored at −80°C.

General techniques. PCR amplifications, cloning procedures, isolation of chromosomal DNA, and DNA manipulations were carried out according to standard procedures (18). Cycle sequencing was performed using the CEQ Dye Terminator Cycle Sequencing Quick Start kit (Beckman Coulter), and sequencing reactions were run on an XL2000 Beckman Coulter sequencer. The *Listeria* home page of the Institut Pasteur (http://genolist.pasteur.fr/ListiList/) and the NCBI database (http://www.ncbi.nlm.nih.gov/) were used for sequence comparisons. All oligonucleotides used for PCR amplification were synthesized by Metabion (Martinsried, Germany).

Disruption of *pycA* and lmo1073 in *L. monocytogenes*. The insertion mutants were constructed by using *L. monocytogenes* Sv1/2a EGD-e as the parental strain, using a protocol described previously (16), by inserting a pLSV101 recombinant plasmid harboring specific fragments of the *pycA* or lmo1073 gene into the corresponding gene of *L. monocytogenes* EGD-e (12, 26). Internal (N-terminal) fragments of 286 bp (*pycA*) and 239 bp (lmo1073) were PCR amplified from chromosomal DNA derived from *L. monocytogenes* EGD-e by using the following primer pairs: pycA-BamHI (AAAAAA**GGATCC**GTAGCAAACCGGC), pycA-EcoRI (AACGAAAA**GAATTC**CTTCTTGCTCA), lmo1073-BamHI (TGGTTTAAA**GGATCC**GCCGTAGTT), and lmo1073-EcoRI (TCTGAGC**GAATTC**TGGATAATCATC) (the restriction endonuclease sites are underlined; boldface indicates deviation from the original sequence). The purified PCR products were digested with the corresponding restriction enzymes and cloned via the restriction sites into pLSV101 to yield the mutagenesis plasmids pLSV101-*pycA* and pLSV101-lmo1073. These plasmids were transformed by electroporation into *L. monocytogenes* EGD-e, and insertion mutants (EGD-e/*pycA*::pLSV101 and EGD-e/lmo1073::pLSV101) were selected by growth on erythromycin at 42°C. Insertional mutagenesis of *pycA* and lmo1073 was confirmed by PCR and sequencing. The revertant of the *pycA* insertion mutant (EGD-e/Rev) was obtained by subcultivating the insertion mutant at 30°C without erythromycin. Precise excision of the single plasmid insertion was confirmed by PCR analysis and sequencing.

[U-$^{13}C_6$]glucose incorporation studies. [U-$^{13}C_6$]glucose was purchased from Campro Scientific (Berlin, Germany). Strains EGD-e and EGD-e/*pycA*::pLSV101 were grown overnight in BHI at 37°C and 42°C, respectively. The cells were sedimented and washed with PBS. BHI was supplemented with 2.5 mg/ml [U-$^{13}C_6$]glucose, and Erlenmeyer flasks with 100 ml BHI with [U-$^{13}C_6$]glucose were then inoculated with an aliquot of the cell suspensions to an OD_{600} of 0.1. The cultures were grown at 37°C until OD_{600} = 0.5 and OD_{600} = 1.0. Sodium azide was then added to a final concentration of 10 mM. The cells were centrifuged and washed three times with PBS.

Protein hydrolysis and amino acid derivatization. Bacterial cells (an approximately 10-mg washed wet pellet) were suspended in 0.5 ml of 6 M hydrochloric acid. The mixture was heated at 105°C for 24 h under an inert atmosphere. The hydrolysate was placed on a column of Dowex 50W × 8 (H^+ form; 200 to 400 mesh; 5 by 10 mm). The column was washed twice with 750 μl of water and was developed with 1 ml of 2 M ammonium hydroxide. An aliquot of the eluate was dried under a stream of nitrogen, and the residue was dissolved in 50 μl of dry acetonitrile. A total of 50 μl of *N*-(tert-butyldimethyl-silyl)-*N*-methyl-trifluoroacetamide containing 1% tert-butyl-dimethyl-silylchloride (Sigma) was added. The mixture was kept at 70°C for 30 min. The resulting mixture of tert-butyldimethylsilyl derivatives (TBDMS) of amino acids was used for gas chromatography/mass spectrometry (GC/MS) analysis without further work-up.

Mass spectrometry. GC/MS analysis was performed on a GCMS-QP2010 Plus Gas Chromatograph/Mass Spectrometer (Shimadzu, Duisburg, Germany) equipped with a fused silica capillary column (Equity TM-5; 30 m by 0.25 mm; 0.25-μm film thickness; Supelco, Bellafonte, PA) working with electron impact ionization at 70 eV. Of a solution containing TBDMS amino acids, 1 μl was injected in 1:10 split mode at an interface temperature of 260°C and a helium inlet pressure of 70 kPa. The column was developed at 150°C for 3 min and then with a temperature gradient of 10°C min^{-1} to a final temperature of 260°C that was held for 3 min. Data were collected using GCMSsolution version 2.50 SU3 software (Shimadzu). Selected ion-monitoring experiments were carried out. Samples were analyzed at least three times, and data were processed as described previously (3). The excess of multiple labeled isotopologues was calculated according to the formula $[2 \times (M + 2) + 3 \times (M + 3) + \ldots + n \times (M + n)]/n$, where n is the number of carbon atoms in a given fragment derived from the original amino acid.

[U-^{14}C]aspartate and [^{3}H]oxaloacetate uptake assays. *L. monocytogenes* strains EGD-e and EGD-e/*pycA*::pLSV101 were grown overnight in BHI at 37°C and 42°C, respectively, and subsequently grown in BHI to an OD_{600} of 0.6. Each culture was then harvested by centrifugation at 5,000 rpm for 3 min at 4°C. The pellet was washed three times in transport buffer (50 mM Tris-HCl, pH 7.2, and 20 mM $MgCl_2$) and resuspended in the same buffer. Labeled L-[U-^{14}C]aspartate (0.1 mCi/ml; Hartmann Analytic, Braunschweig, Germany) or [^{3}H]oxaloacetate was added in a final concentration of 10 mM and incubated at 37°C. Aliquots were retrieved at different time points and filtered rapidly under vacuum through a 0.45-μm-pore-size cellulose nitrate filter (Sartorius, Göttingen, Germany). The filters were washed with 9 ml cold 0.9% NaCl and dried for 20 min at 42°C. Radioactivity was determined using a Perkin-Elmer 1214 Rackbeta liquid scintillation counter. Additionally, the CFU of each sample were determined, and the glucose uptake was calculated for each strain.

Transcriptome analyses. Transcriptome analyses were performed using whole-genome DNA microarrays as described by Marr et al. (14). Two independently isolated RNA samples from the wild-type *L. monocytogenes* EGD-e and the *pycA* insertion mutant grown in BHI to an OD_{600} of 1.0, were used for the analysis. Each RNA pair was reverse transcribed and hybridized to two microarray slides with dye swap. Another two microarray slides were hybridized using the same principle. In total, four microarray slides to generate 16 replicate expression values were used for further analysis. cDNA labeling and hybridization were performed as described previously (14). The slides were scanned using ScanArray HT and analyzed using Scan-Array express software (Perkin-Elmer, Boston, MA). Spots were flagged and eliminated from analysis when the signal-to-noise ratio was less than 3 or in obvious instances of high background or stray fluorescent signals. The LOWESS method of normalization (27) was performed on the background-corrected median intensity of the spots. The normalized ratios were analyzed further with Microsoft Excel (Microsoft, Redmond, WA) and SAM (significance analysis of microarrays) software for statistical significance (http://www-stat.stanford.edu/~tibs/SAM/). As described previously (16), genes whose expression values were >2.0 or <0.5 were considered to be differentially regulated. The data discussed in this work are listed in Table 1.

Cell infection assays. Human colon epithelial cells (Caco-2; ACC 169) and mouse monocytes/macrophages (J774A.1; ACC 170) were received from the German Collection of Microorganisms and Cell Cultures (DMSZ) and cultured at 37°C and 5% CO_2 in RPMI 1640 medium supplemented with 2 mM L-glutamine (Gibco, Eggenstein, Germany) and 10% heat-inactivated fetal calf serum (FCS) (Biochrom KG, Berlin, Germany). A total of 1×10^5 Caco-2 or J774A.1 cells per well were seeded in 24-well culture plates 24 h prior to infection. The cells were washed twice with phosphate-buffered saline (PBS) supplemented with Mg^{2+} Ca^{2+} (PBS-Mg^{2+} Ca^{2+}) and infected at a multiplicity of infection (MOI) of 10 bacteria per cell for 1 h (Caco-2) or an MOI of 1 for 45 min (J774A.1). The cells were washed with PBS-Mg^{2+} Ca^{2+} at time zero (t = 0 h) and incubated with medium containing 50 μg/ml gentamicin, which was replaced with medium containing 10 μg/ml gentamicin after 1 h. Cells were washed and lysed at appropriate time points using cold distilled water, and viable bacterial counts of intracellular bacteria were determined by plating serial dilutions on BHI agar plates.

Infection of mice. Six- to 12-week-old female C57BL/6 mice were purchased from Harlan Winkelmann GmbH, Borchen, Germany. The animals were housed under specific-pathogen-free conditions at the Biocenter of the University of Würzburg. All animal experiments were approved by the government of Unterfranken and were performed according to the German animal protection guidelines. Groups of five mice were intravenously infected for immunization with 5×10^3 bacteria unless otherwise noted and resuspended in 0.1 ml endotoxin-free 0.9% NaCl. Three days postinfection, the spleens and livers of the mice were harvested for determination of the number of *L. monocytogenes* bacteria in the lysates of the infected spleens and livers. Counts of viable intracellular bacteria were determined by plating serial dilutions of mechanically lysed cell suspensions on BHI agar.

Microarray data accession number. The complete microarray data set associated with this study has been deposited in NCBI's Gene Expression Omnibus (GEO) (http://www.ncbi.nlm.nih.gov/geo/) and is accessible through accession number GSE19014.

RESULTS

Construction and characterization of a *pycA* insertion mutant of *L. monocytogenes* EGD-e. The PYC-mediated synthesis of oxaloacetate appears to be an important anaplerotic reaction in *L. monocytogenes* leading to C_4 metabolites, and hence, the enzyme may play a crucial role in *L. monocytogenes* carbon metabolism. The present study aimed to analyze the significance of PYC in the listerial metabolism under extra- and intracellular growth conditions and the effect of PYC deficiency on *in vivo* virulence. For this goal, a *pycA* insertion mutant (EGD-e/*pycA*::pLSV101) was constructed. Attempts to construct an in-frame deletion of *pycA* using a conditionally replicating plasmid (12) failed, probably because the *pycA* mutant was overgrown by the wild-type strain (see below) in the absence of a selective marker. The *pycA* insertion mutant grew at a 2- to 3-fold-lower rate than the wild-type strain, EGD-e, when cultured in BHI broth (Fig. 1A) but was completely unable to multiply in a defined minimal medium (17) with glucose or glycerol as a carbon source (Fig. 1B and C).

To ensure that the observed phenotype of the *pycA* mutant was exclusively caused by the inactivation of the *pycA* gene, we isolated a revertant strain, EGD-e/Rev, that had the pSLV101-*pycA* insertion precisely excised, as confirmed by DNA sequencing. Spontaneous excision of the insertion occurs in the absence of selection pressure at a rate of approximately 10^{-7} and restores in most cases the wild-type genotype without mutations (5, 12). Repeatedly isolated revertants grew in all the culture media used at rates similar to that of the wild-type strain (Fig. 1B), ruling out an additional mutation(s) that might be responsible for the failure of the *pycA* mutant to grow in the defined minimal medium. Since *pycA* is constitutively expressed under all culture conditions (11), we assumed that the use of the revertant strain as a control was superior to *trans* complementation by a recombinant *pycA*-carrying plasmid, which, due to the higher *pycA* copy number, would probably lead to elevated PYC activity in the complemented *pycA* mutant with unpredictable consequences for metabolism. Indeed, complementation of the *pycA* mutant with two recombinant plasmids (pAD123-*pycA* and pHSP9-*pycA*) could not be demonstrated by either of these recombinant plasmids when the strains were grown in liquid medium. However, growth of the EGD-e wild-type strain carrying the recombinant *pycA* plasmids was strikingly inhibited, demonstrating adverse effects on carbon metabolism by both recombinant plasmids, possibly due to an unbalanced PycA concentration or involvement of noncoding RNA (data not shown).

The *pycA* gene (lmo1072) is the first gene of a transcription unit that contains three additional genes (lmo1073 to lmo1075) located downstream. The insertion of pLSV101 into *pycA* may therefore cause a polar effect on the expression of these genes. Microarray analysis indeed showed a significantly smaller amount of transcript of the first downstream gene, lmo1073, compared to the wild-type strain (Table 1, note *e*), while the transcription of the gene lmo1071, located upstream, was unaffected by the insertion in *pycA*. To test whether the lower expression of lmo1073, encoding a putative metal binding protein of an ABC transporter, may be responsible for the growth defect of the *pycA* insertion in the defined growth medium, we constructed an insertion mutant of lmo1073 using the same strategy as for *pycA*. The resulting mutant, EGD-e/lmo1073::pLSV101, grew in BHI at a rate similar to that of the wild-type strain and showed only slight growth inhibition compared to the wild-type strain in the above-described defined minimal medium containing glucose or glycerol (Fig. 1A to C).

These results rule out the possibility that the transcriptional impairment of lmo1073 or of the genes located further downstream, lmo1074 and lmo1075, due to the pLSV101 insertion in *pycA* is responsible for the growth defect of the *pycA* insertion mutant, but they suggest that this failure is caused entirely by the inactivation of PYC. We therefore conclude that the PYC-mediated anaplerotic reaction resulting in the production of oxaloacetate is essential during growth of *L. monocytogenes* in a culture medium where carbon and energy metabolism depends entirely on the carbon source added.

Oxaloacetate cannot be produced in the *pycA* mutant by alternative reactions. As the *pycA* mutant was still able to grow

TABLE 1. Transcriptome analysis of EGD-e/*pycA*::pLSV101

Gene[a]	Encoded protein	Relative transcript level
Downregulated		
lmo0048	Similar to *Staphylococcus* two-component sensor histidine kinase AgrB	0.02
lmo0049	Unknown	0.02
lmo0050	Similar to sensor histidine kinase (AgrC from *Staphylococcus*)	0.02
lmo0051	Similar to 2-component response regulator protein (AgrA from *Staphylococcus*)	0.02
lmo0208	Conserved hypothetical protein	0.47
lmo0210 (*ldh*)	Similar to L-lactate dehydrogenase	0.19
lmo0238 (*cysE*)	Similar to serine *O*-acetyltransferase	0.31
lmo0239 (*cysS*)	Cysteinyl-tRNA synthetase	0.33
lmo0240	Highly similar to *B. subtilis* YazC protein	0.35
lmo0241	Similar to conserved hypothetical proteins like *B. subtilis* YacO protein	0.34
lmo0242	Similar to *B. subtilis* YacP protein	0.40
lmo0243 (*sigH*)	RNA polymerase σ^{30} factor	0.44
lmo0283	Similar to ABC transporter permease protein	0.34
lmo0284	Similar to ABC transporter (ATP-binding protein)	0.38
lmo0285	Putative lipoprotein	0.41
lmo0286	Similar to aminotransferase	0.34
lmo0302	Unknown	0.35
lmo0352	Highly similar to regulatory proteins (DeoR family)	0.44
lmo0477	Putative secreted protein	0.02
lmo0478	Putative secreted protein	0.02
lmo0479	Putative secreted protein	0.03
lmo0560[d]	Similar to NADP-specific glutamate dehydrogenase	0.30
lmo0641	Similar to heavy metal-transporting ATPase	0.25
lmo0642	Unknown	0.25
lmo0778	Unknown	0.13
lmo0780	Unknown	0.44
lmo0788	Unknown	0.31
lmo0795	Conserved hypothetical protein	0.45
lmo1014 (*gbuA*)[b]	Highly similar to glycine betaine ABC transporter (ATP-binding protein)	0.44
lmo1015 (*gbuB*)[b]	Highly similar to glycine betaine ABC transporters (permease)	0.43
lmo1056	Unknown	0.52
lmo1073[b]	Similar to metal binding protein (ABC transporter)	0.14
lmo1120	Unknown	0.53
lmo1121	Unknown	0.55
lmo1227	Similar to uracil-DNA glycosylase	0.42
lmo1298 (*glnR*)[e]	Similar to glutamine synthetase repressor	0.15
lmo1299 (*glnA*[e]	Highly similar to glutamine synthetases	0.21
lmo1516[d]	Similar to ammonium transporter NrgA	0.10
lmo1517[d]	Similar to nitrogen regulatory PII protein	0.16
lmo1634	Similar to alcohol-acetaldehyde dehydrogenase	0.11
lmo1983 (*ilvD*)	Similar to dihydroxy-acid dehydratase	0.39
lmo1984 (*ilvB*)[b]	Similar to acetolactate synthase (acetohydroxy-acid synthase) (large subunit)	0.49
lmo1985 (*ilvN*)[b]	Similar to acetolactate synthase (acetohydroxy-acid synthase) (small subunit)	0.41
lmo2064	Similar to large conductance mechanosensitive channel protein	0.34
lmo2192[d]	Similar to oligopeptide ABC transporter (ATP-binding protein)	0.40
lmo2193[d]	Similar to oligopeptide ABC transporter (ATP-binding protein)	0.48
lmo2195[d]	Similar to oligopeptide ABC transporter (permease)	0.45
lmo2360	Transmembrane protein	0.49
lmo2374	Similar to aspartate kinase	0.49
lmo2407	Unknown	0.53
lmo2410[e]	Unknown	0.26
lmo2457 (*tpi*)[d]	Highly similar to triose phosphate isomerase	0.42
lmo2458 (*pgk*)[d]	Highly similar to phosphoglycerate kinase	0.38
lmo2459 (*gap*)[d]	Highly similar to glyceraldehyde 3-phosphate dehydrogenase	0.34
lmo2460[d]	Similar to *B. subtilis* CggR hypothetical transcriptional regulator	0.18
lmo2587	Conserved hypothetical protein	0.41
lmo2646	Unknown	0.02
lmo2648	sImilar to phosphotriesterase	0.02
lmo2753[e]	Unknown	0.43
lmo2761	Similar to β-glucosidase	0.03
lmo2762	Similar to PTS cellobiose-specific enzyme IIB	0.10
lmo2763	Similar to PTS cellobiose-specific enzyme IIC	0.12
lmo2764	Similar to xylose operon regulatory protein and to glucose kinase	0.12
lmo2768	Hypothetical membrane protein	0.45
lmo2785 (*kat*)[e]	Catalase	0.46
lmo2857	Hypothetical protein	0.32

Continued on following page

TABLE 1—*Continued*

Gene[a]	Encoded protein	Relative transcript level
Upregulated		
lmo0109[b]	Similar to transcriptional regulatory proteins, AraC family	5.14
lmo0110[c]	Similar to lipase	3.83
lmo0130[d]	Similar to 5-nucleotidase, putative peptidoglycan bound protein (LPXTG motif)	14.16
lmo0135[d]	Similar to oligopeptide ABC transport system substrate-binding proteins	3.40
lmo0211 (*ctc*)	Similar to *B. subtilis* general stress protein	2.32
lmo0267	Similar to other proteins	1.85
lmo0391[b]	Unknown	2.25
lmo0392[b]	Highly similar to *B. subtilis* YqfA protein	2.09
lmo0422[b]	Similar to unknown protein	1.95
lmo0514	Similar to internalin protein, putative peptidoglycan bound protein (LPXTG motif)	2.26
lmo0530	Unknown	2.30
lmo0556[b]	Similar to phosphoglycerate mutase	2.31
lmo0715	Unknown	2.09
lmo0769	Similar to α-1,6-mannanase	3.81
lmo0863	Unknown	2.57
lmo0864	Unknown	3.56
lmo0865	Similar to phosphomannomutase	2.52
lmo0971 (*dltD*)	DltD protein for D-alanine esterification of lipoteichoic acid and wall teichoic acid	2.22
lmo0972 (*dltC*)	D-Alanyl carrier protein	1.94
lmo0973 (*dltB*)	DltB protein for D-alanine esterification of lipoteichoic acid and wall teichoic acid	2.08
lmo0974 (*dltA*)[c]	D-Alanine-activating enzyme (Dae), D-alanine-D-alanyl carrier protein ligase (Dcl)	2.11
lmo1042[b]	Similar to molybdopterin biosynthesis protein MoeA	2.60
lmo1043	Similar to molybdopterin-guanine dinucleotide biosynthesis MobB	2.56
lmo1044[b]	Similar to molybdopterin converting factor, subunit 2	2.89
lmo1045[b]	Similar to molybdopterin converting factor, subunit 1	2.77
lmo1046[b]	Similar to molybdenum cofactor biosynthesis protein C	3.07
lmo1047	Similar to molybdenum cofactor biosynthesis protein A	2.37
lmo1048[b]	Similar to molybdenum cofactor biosynthesis protein B	1.95
lmo1049	Similar to molybdopterin biosynthesis protein MoeB	2.92
lmo1097	Similar to integrases	2.81
lmo1142	Similar to *Salmonella enterica* PduS protein	3.73
lmo1143	Similar to *S. enterica* PduT protein	3.56
lmo1144	Similar to *S. enterica* PduU protein	2.29
lmo1145	Similar to *S. enterica* PduV protein	2.37
lmo1146	Unknown	2.44
lmo1150	Regulatory protein similar to *S. enterica* serovar Typhimurium PocR protein	7.31
lmo1172[b]	Similar to two-component response regulator	10.10
lmo1254[d]	Similar to α,α-phosphotrehalase	7.38
lmo1255[d]	Similar to PTS system trehalose-specific enzyme IIBC	9.42
lmo1306	Highly similar to *B. subtilis* YneF protein	2.52
lmo1339	Similar to glucose kinase	1.99
lmo1349[b]	Similar to glycine dehydrogenase (decarboxylating) subunit 1	4.21
lmo1388 (*tcsA*)[d]	$CD4^+$ T-cell-stimulating antigen, lipoprotein	2.41
lmo1396	Similar to phosphatidylglycerophosphate synthase	1.94
lmo1416	Unknown	2.83
lmo1425 (*opuCD*)	Similar to betaine/carnitine/choline ABC transporter	1.90
lmo1521	Similar to *N*-acetylmuramoyl-L-alanine amidase	2.45
lmo1538[b]	Similar to glycerol kinase	4.35
lmo1539[b]	Similar to glycerol uptake facilitator	5.31
lmo1648	Unknown	2.65
lmo1690	Similar to hypothetical proteins	4.01
lmo1879 (*cspD*)[b]	Similar to cold shock protein	11.39
lmo1883[b]	Similar to chitinases	8.00
lmo1900 (*panD*)	Similar to aspartate 1-decarboxylases	3.86
lmo1901 (*panC*)	Similar to panthotenate synthetases	3.68
lmo1902 (*panB*)	Similar to ketopantoate hydroxymethyltransferases	5.94
lmo1903	Similar to thioredoxin	2.47
lmo1954 (*drm*)	Similar to phosphopentomutase	3.92
lmo1955[b]	Similar to integrase/recombinase	3.04
lmo1970	Similar to putative phosphotriesterase-related proteins	2.78
lmo1972	Similar to pentitol PTS system enzyme IIB component	4.53
lmo1974	Similar to transcription regulators (GntR family)	2.87
lmo1999[b]	Weakly similar to glucosamine-fructose-6-phosphate aminotransferase	2.14
lmo2007	Weakly similar to putative sugar-binding lipoproteins	2.10
lmo2084[d]	Unknown	2.66

Continued on following page

TABLE 1—*Continued*

Gene[a]	Encoded protein	Relative transcript level
lmo2104	Unknown	2.42
lmo2257	Hypothetical CDS	16.96
lmo2293[d]	Protein gp10 (bacteriophage A118)	6.05
lmo2295[d]	Protein gp8 (bacteriophage A118)	7.76
lmo2296[d]	Similar to coat protein (bacteriophage SPP1)	13.00
lmo2298[d]	Protein gp4 (bacteriophage A118)	12.60
lmo2300	Putative terminase large subunit (bacteriophage A118)	6.06
lmo2304	Protein gp65 (bacteriophage A118)	3.61
lmo2305	Unknown	2.63
lmo2306	Similar to phage protein	3.61
lmo2307	Hypothetical protein	4.35
lmo2308	Similar to single-stranded DNA-binding protein	3.72
lmo2309	Unknown	2.58
lmo2310	Unknown	3.71
lmo2311	Unknown	3.97
lmo2312	Unknown	4.29
lmo2315	Similar to protein gp51 (bacteriophage A118)	2.92
lmo2322	Protein gp44 (bacteriophage A118)	3.20
lmo2335 (*fruA*)	Highly similar to PTS fructose-specific enzyme IIABC component	54.79
lmo2336 (*fruB*)	Fructose-1-phosphate kinase	98.99
lmo2337	Similar to regulatory protein DeoR family	112.00
lmo2343	Similar to nitrilotriacetate monooxygenase	2.74
lmo2344	Similar to *B. subtilis* YtnI protein	2.97
lmo2345	Conserved hypothetical protein	2.56
lmo2437[d]	Unknown	10.25
lmo2522	Similar to hypothetical cell wall binding protein from *B. subtilis*	3.30
lmo2539 (*glyA*)	Highly similar to glycine hydroxymethyltransferase	2.20
lmo2590[b]	Similar to ATP binding proteins	4.55
lmo2684[c]	Similar to cellobiose phosphotransferase enzyme IIC component	18.73
lmo2685[c]	Similar to cellobiose phosphotransferase enzyme IIA component	17.18
lmo2708	Similar to PTS system, cellobiose-specific enzyme IIC	17.05
lmo2714	Peptidoglycan-anchored protein (LPXTG motif)	2.10
lmo2742[d]	Unknown	6.51
lmo2743	Similar to transaldolase	6.06
lmo2771[b]	Similar to β-glucosidase	135.36
lmo2772[b]	Similar to β-glucoside-specific enzyme IIABC	207.92
lmo2773[b]	Similar to transcription antiterminator	178.03
lmo2786 (*bvrC*)	Unknown	2.93
lmo2787 (*bvrB*)[b]	β-Glucoside-specific phosphotransferase enzyme IIABC component	10.06
lmo2788 (*bvrA*)[b]	Transcription antiterminator	4.51
lmo2797[b]	Similar to phosphotransferase system mannitol-specific enzyme IIA	5.61
lmo2798[b]	Similar to phosphatase	6.56
lmo2851	Similar to AraC-type regulatory protein	4.98

[a] Genes were identified by microarray analyses as down- or upregulated in EGD-e/*pycA*::pLSV101 relative to *L. monocytogenes* EGD-e grown in BHI medium.
[b] Gene or operon whose transcription was shown previously to be controlled by CcpA and Hpr-SerP (16).
[c] Gene or operon whose transcription was shown previously to be controlled by CcpA only (16).
[d] Gene or operon whose transcription was shown previously to be controlled by Hpr-SerP only (16).
[e] Gene or operon whose transcription was shown previously to be controlled by reduced glucose uptake (14, 16).

in BHI, it might be argued that oxaloacetate is produced in the *pycA* mutant by an alternative metabolic reaction(s) catalyzed by yet-undefined enzymes that are expressed and/or activated in BHI, thus replacing PYC. To test this hypothesis, the wild-type strain and the *pycA* mutant were cultured in BHI supplemented with uniformly ^{13}C-labeled glucose ([U-$^{13}C_6$]glucose), and ^{13}C incorporation into protein-derived aspartate, glutamate, and alanine was analyzed by mass spectrometry as described previously (3). As shown in Fig. 2, incorporation of ^{13}C was not detectable in aspartate and glutamate derived from EGD-e/*pycA*::pLSV101 that was harvested in two different growth phases, namely, at OD_{600} = 0.5 and 1.0. However, high ^{13}C incorporation into both amino acids of proteins of the wild-type strain cultivated under the same conditions was observed. Oxaloacetate is the direct precursor of the biosynthesis of aspartate and is also needed for the production of oxoglutarate (via the citrate cycle) as the precursor of glutamate. ^{13}C incorporation from [U-$^{13}C_6$]glucose into alanine, used as a control, was similar in the *pycA* mutant and the wild-type strain (Fig. 2), indicating that the production of the glycolytic intermediate pyruvate, the precursor of alanine, is unaffected by the *pycA* mutation. The clear difference of ^{13}C enrichment in aspartate and its precursor, oxaloacetate, between the wild-type and the mutant strain shows that the PYC-catalyzed anaplerotic reaction is indeed the predominant reaction leading to oxaloacetate production in *L. monocytogenes.*

Growth of the *pycA* mutant in defined minimal medium cannot be restored by supplementation with oxaloacetate or aspartate. Several growth and transport experiments were performed with the wild-type strain and the *pycA* mutant. Addi-

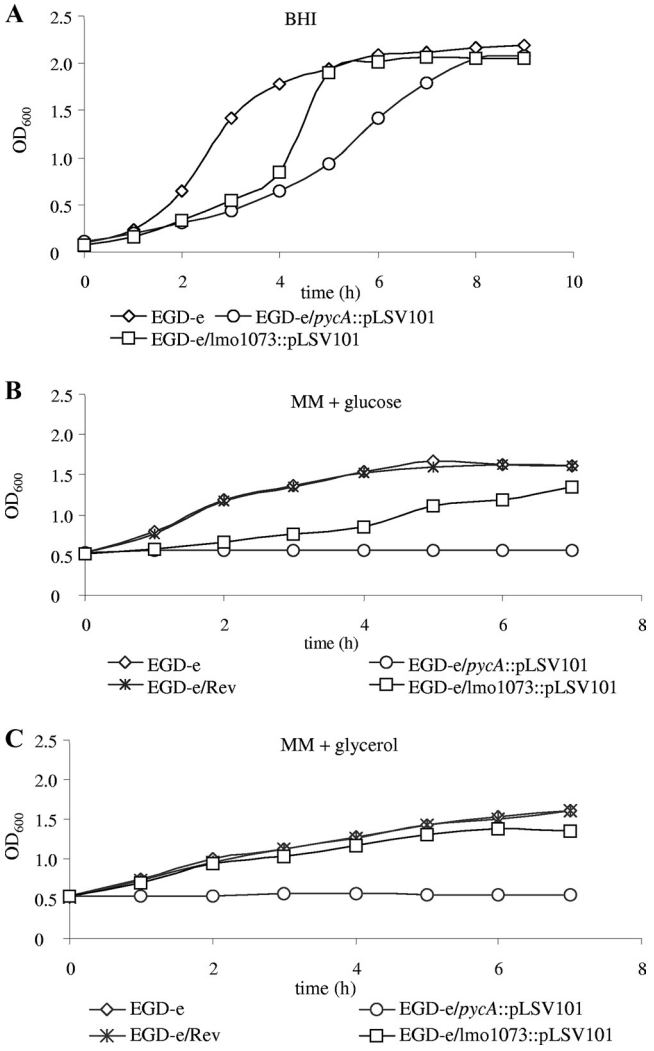

FIG. 1. (A) Growth of *L. monocytogenes* EGD-e, EGD-e/*pycA*::pLSV101, and EGD-e/lmo1073::pLSV101 in BHI. (B and C) Growth of *L. monocytogenes* EGD-e, EGD-e/*pycA*::pLSV101, the revertant of the *pycA* insertion mutant (EGD-e/Rev), and EGD-e/lmo1073::pLSV101 in MM supplemented with 50 mM glucose (MM + glucose) or 50 mM glycerol (MM + glycerol). The strains were first grown in BHI medium to an OD_{600} of 0.5. After centrifugation, the cells were washed twice with MM and then resuspended in MM with the appropriate carbon source. All growth curves are representative of three replicates.

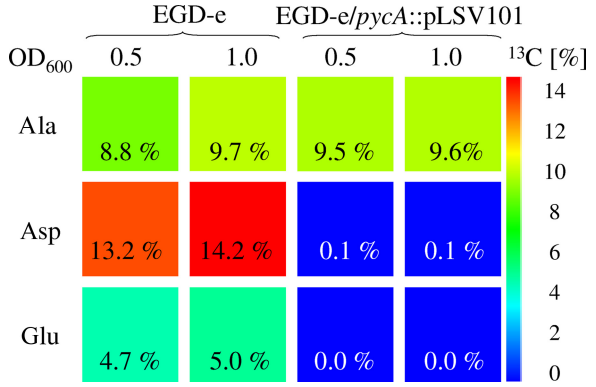

FIG. 2. ^{13}C excess (percent) from [U-$^{13}C_6$]glucose of multiply labeled isotopologues of alanine (Ala), aspartate (Asp), and glutamate (Glu) derived from bacterial protein. The color map indicates ^{13}C excess on a linear scale.

tion of oxaloacetate or aspartate at concentrations between 1 and 10 mM to the glucose- or glycerol-containing minimal medium could not restore growth of the *pycA* mutant. External oxaloacetate could not be transported into the listerial cell, as shown by the lack of uptake of ^{3}H-labeled oxaloacetate by either the wild-type strain or the *pycA* mutant (data not shown). This was expected, as the *L. monocytogenes* genome apparently lacks a gene(s) for oxaloacetate (and other C_4 dicarboxylate) permease(s) (7). In contrast, ^{14}C-labeled aspartate is taken up by the *pycA* mutant at a rate similar to that by the wild-type strain (Fig. 3) but is apparently not efficiently converted into oxaloacetate. The addition of 1% CAA, which contain all amino acids except tryptophan, or of CAA and malate, succinate, and oxaloacetate to the minimal medium only partially restored the growth of the *pycA* mutant (Fig. 4A and B). This indicates that the lack not only of synthesis of the amino acids belonging to the aspartate family, but also of other reactions involving oxaloacetate (e.g., the conversion to other C_4 dicarboxylates) may be responsible for the poor growth of the *pycA* mutant under these conditions.

Comparative transcript profiles of the *pycA* mutant and the wild-type strain. The supply of carbon substrates present in BHI is obviously richer than that in the defined medium and allows rather efficient growth of the *pycA* mutant. To find out which metabolic pathway(s) may enable the *pycA* mutant to grow in BHI, comparative transcript profiling of the *pycA* mutant and the EGD-e wild-type strain was performed. For this purpose, RNAs of the two strains, grown in BHI to an OD_{600} of 1.0, where both strains were still in the logarithmic growth phase (Fig. 1), was used. In total, 174 genes were found to be differentially expressed (Table 1), 108 were significantly upregulated (>2-fold), and 66 were downregulated (<0.5-fold) in the *pycA* mutant in comparison to strain EGD-e.

Among the downregulated genes, the most pronounced were those encoding the two-component AgrAB(C) system and the major transcription regulator of glycolysis, CggR. Con-

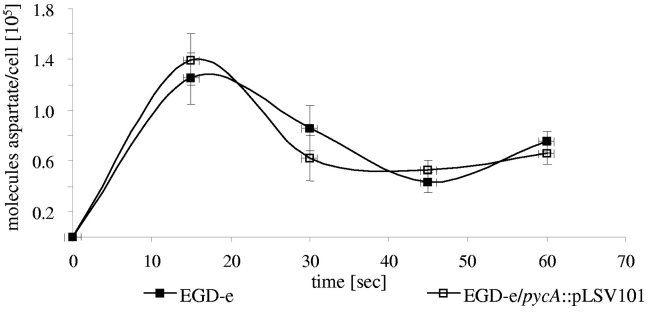

FIG. 3. [U-^{14}C]aspartate uptake rate in wild-type *L. monocytogenes* EGD-e and EGD-e/*pycA*::pLSV101. The strains were pregrown in BHI to an OD_{600} of 0.6. The *y* axis indicates the number of aspartate molecules taken up per bacterial cell. The aspartate uptake measurements were performed in triplicate, and the error bars indicate the standard deviations from the means.

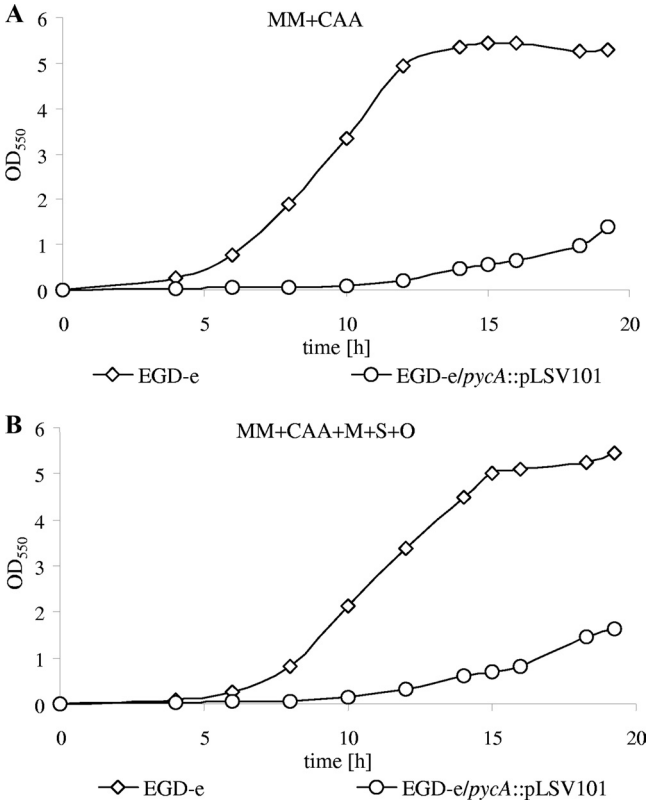

FIG. 4. Strains EGD-e and EGD-e/*pycA*::pLSV101 were grown overnight in BHI and diluted 1:400 in MM containing 1% CAA (A) and 1% CAA, 1 g/liter malate, 1 g/liter succinate, and 1 g/liter oxaloacetate (B). Bacterial growth was monitored at OD_{550} for 20 h. The average values of three independent experiments are shown.

comitantly with the reduced level of CggR, the *gap* operon encoding enzymes of the glycolysis pathway, especially *tpi*, *pgk*, and *gap*, was also downregulated (downregulation of *eno* and *pgm* was less reproducible), suggesting reduced glucose catabolism in the *pycA* mutant.

In line with this assumption, most of the differentially regulated genes of the *pycA* mutant marked in Table 1 are under positive or negative glucose control by CcpA-dependent and -independent mechanisms in *L. monocytogenes* and *Bacillus subtilis* (6, 14). Exceptions among the downregulated genes include the aspartate kinase gene, an operon for a cellobiose-specific PTS, the *agrABC* operon (lmo0048 to lmo0051), and lmo0477 to lmo0479. The function of the *L. monocytogenes*-specific genes is presently unknown. Among the upregulated genes whose expression does not seem to be under direct glucose control are several genes with unknown functions, lmo2335 to lmo2337 (*fruRAB*), encoding a PTS^{Fru}; *panBCD* (lmo1900 to lmo1902), involved in panthotenate biosynthesis; lmo0769 and lmo0865, encoding α-1,6-mannanase and phosphomannomutase, respectively; and several genes involved in cell wall biosynthesis, such as the *dlt* operon, lmo1521, and lmo2522. The upregulation of these genes may point to a special need for the encoded pathways and enzymes when the *pycA* mutant grows in BHI.

Many of the glucose-controlled genes whose transcription is significantly upregulated in the *pycA* mutant encode reactions and pathways involved in carbon metabolism. These genes include lmo0135, encoding a component of a putative oligopeptide ABC transporter; lmo1538 and lmo1539, encoding a glycerol kinase and a glycerol uptake facilitator essential for glycerol metabolism; the operons lmo1042 to lmo1049 and lmo1144 to lmo1150, involved in vitamin B_{12} synthesis and the vitamin B_{12}-dependent propanediol utilization (Pdu) pathway, respectively; and lmo1349, encoding a glycine dehydrogenase. High upregulation is observed for the operons encoding several PTS permeases, lmo1255, lmo2683 to lmo2685, lmo2771 to lmo2773, and lmo2786 to lmo2788 (*bvrCBA*). In *L. monocytogenes*, the expression of these PTS operons appears to be regulated by PTS regulation domain-containing antiterminators and activators (22a) that may be activated by low glucose concentrations (23).

The *pycA* mutant is taken up by mammalian cells but is unable to replicate in these host cells, and its virulence is attenuated in the mouse. To test whether the *pycA* mutant encounters within mammalian host cells growth conditions similar to those in rich medium (BHI) or in the nutrient-limited defined culture media, we determined the intracellular replication of the *pycA* mutant in the macrophage-like J774A.1 cells and in the epitheloid Caco-2 cells (Fig. 5A and B). The *pycA* mutant was taken up by both cell types with efficiencies that were about 5-fold lower in the macrophages and almost 100-fold lower in the Caco-2 cells than those of the EGD-e wild-type strain. However, subsequent replication of the *pycA* mutant in the host cells did not occur, indicating that the host cell is unable to compensate for the lack of PYC-mediated oxaloacetate production of the *pycA* mutant. The *pycA* revertant strain EGD-e/Rev was again able to replicate in the cytosol with efficiency similar to that of the wild-type strain. Mutant EGD-e/lmo1073::pLSV101, used as a control, could still replicate in both host cell types at only a slightly lower rate (Fig. 5A and B). These data clearly show that the PYC-catalyzed production of oxaloacetate is also indispensable for the intracellular replication of *L. monocytogenes*.

To determine whether and to what extent the virulence of the *pycA* mutant is attenuated in the mouse sepsis model, 5×10^3 EGD-e/*pycA*::pLSV101 cells were injected into the tail veins of C57BL/6 mice. As controls, an equal number of EGD-e and mutant EGD-e/lmo1073::pLSV101 bacteria were injected in parallel into C57BL/6 mice. Counts of viable bacteria were determined in the livers and spleens 3 days after intravenous infection. As shown in Fig. 6, the wild-type and EGD-e/lmo1073::pLSV101 strains multiplied up to 10^6 and 10^7 viable counts in the livers and spleens, respectively, 3 days postinfection, as reported previously (15), whereas no counts of viable EGD-e/*pycA*::pLSV101 bacteria could be detected in either the livers or spleens of the infected mice. This result shows that the virulence of the *pycA*-deficient mutant is highly attenuated, and it is apparently unable to reach these organs. Mice infected with up to 5×10^7 EGD-e/*pycA*::pLSV101 cells showed still lower counts of viable bacteria in livers and spleens than mice infected with a number of wild-type bacteria 4 orders of magnitude lower. Even with this high dose of intravenously injected *pycA* mutant bacteria, the infected mice not only survived, but showed no sign of disease.

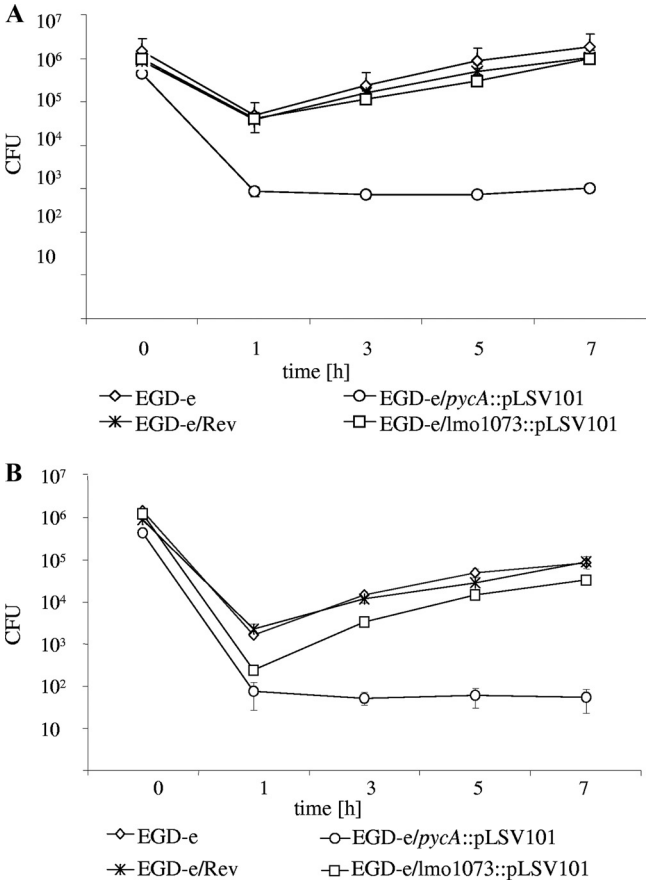

FIG. 5. Effect of the pLSV101 insertion in the *pycA* gene on the intracellular replication of *L. monocytogenes*. J774.A1 (A) and Caco-2 (B) cells were infected with either EGD-e, the *pycA* insertion mutant (EGD-e/*pycA*::pLSV101), or the revertant of the *pycA* insertion mutant (EGD-e/Rev), and the numbers of bacteria recovered at various time points ($t = 0$ h, $t = 1$ h, $t = 3$ h, $t = 5$ h, and $t = 7$ h) after infection were determined as described in Materials and Methods. Three independent infections were performed for each strain, and the error bars indicate the standard deviations from the means.

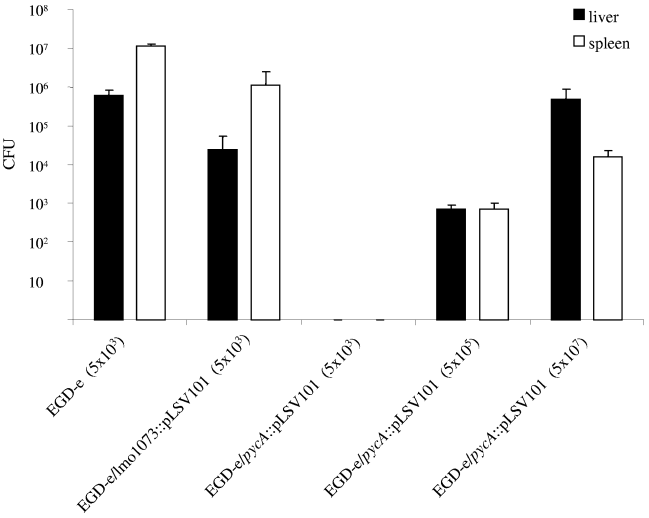

FIG. 6. Viable bacterial counts in spleens and livers of C57BL/6 mice 72 h after intravenous infection with 5×10^3 CFU of *L. monocytogenes* EGD-e and the lmo1073 insertion mutant (EGD-e/lmo1073::pLSV101) or with 5×10^3, 5×10^5, and 5×10^7 CFU of EGD-e/*pycA*::pLSV101. Each bar represents the infection experiments on a group of five animals, and the error bars indicate the standard deviations from the means.

DISCUSSION

Oxaloacetate plays a central role in the bacterial carbon metabolism (19). It acts as a direct precursor for the biosyntheses of aspartate/asparagine, lysine, threonine, and β-alanine (pantothenate) and indirectly for the biosyntheses of arginine, histidine, purine, nicotinate, and nicotinamide. As an acceptor for acetyl-CoA, it coinitiates the citrate cycle and hence is essential for the generation of additional important intermediates, such as succinyl-CoA and 2-oxoglutarate, the precursor of glutamate/glutamine, proline, and arginine. In most heterotrophic bacteria, including pathogens, the generation of oxaloacetate is safeguarded by the presence of several reactions. In addition to the (complete) citrate cycle, several anaplerotic reactions can produce oxaloacetate, including pyruvate and PEP carboxylases, as well as the often reversible PEP carboxykinase.

For example, *B. subtilis*, phylogenetically related to *L. monocytogenes*, possesses a complete citrate cycle and, in addition, PYC and a bifunctional PEP carboxykinase, which ensures the robustness of mutations around the pyruvate node (28). In contrast, *L. monocytogenes* is characterized by an interrupted citrate cycle that is unable to generate oxaloacetate (2), and only a *pycA* gene (lmo1072) encoding PYC, but no *pckA* gene for a PEP carboxykinase, was identified in the *L. monocytogenes* genome (7).

As shown in this study, PYC-mediated pyruvate carboxylation is the predominant reaction providing oxaloacetate when *L. monocytogenes* grows on a single carbon substrate that serves as the source for energy and all catabolic intermediates. This is a rather unusual situation even among intracellular bacterial pathogens, all of which, with the exception of *Chlamydia*, produce oxaloacetate via a complete citrate cycle and, in addition, by PYC and/or PEP carboxylase.

No major alternative reaction leading to oxaloacetate besides pyruvate carboxylation seems to exist in *L. monocytogenes*. The *pycA* mutant characterized in this study was obtained by the insertion of an erythromycin resistance (Em^r) plasmid into the *pycA* gene. Our data show that the growth failure of this mutant is caused by the inactivated PYC and not by polar effects on the genes located up- or downstream. Accidental mutations in the *pycA* mutant affecting its growth can also be excluded, since a revertant strain with the insertion precisely excised grew in glucose-containing defined medium at a rate comparable to that of the wild-type strain.

The lack of ^{13}C incorporation into aspartate and glutamate in the *pycA* mutant growing in BHI in the presence of uniformly labeled [^{13}C]glucose shows that there is no induction of an alternative oxaloacetate-generating reaction in the mutant. The recently reported predominant generation of $^{13}C_3$-labeled aspartate in *L. monocytogenes* growing in J774 macrophages in the presence of uniformly labeled [^{13}C]glucose is also in line with this conclusion (3).

The failure to restore the growth of the *pycA* mutant by addition of oxaloacetate to the defined minimal medium is

apparently due to the lack of a transporter for oxaloacetate. The *L. monocytogenes* genome sequence (7) indeed lacks the genes for either a DctA homologue, known to transport C_4 dicarboxylates in several Gram-positive and Gram-negative bacteria (9), or a CitM homologue, which, besides citrate, can also transport C_4 dicarboxylates (7, 25).

Aspartate, on the other hand, is efficiently taken up by the *pycA* mutant, probably by the gene products of lmo0847 and lmo1740, encoding putative GltK-homologous ABC transporters for glutamate/aspartate. Nevertheless, even an excess of aspartate cannot restore the growth defect of the *pycA* mutant in minimal medium. Aspartate can be converted to oxaloacetate by either aspartate aminotransferase or aspartate oxidase. The genes for both enzymes, *aspB* (lmo1897) and *nadB* (lmo2023), have been identified in the *L. monocytogenes* genome (7). Aspartate aminotransferase uses mainly 2-oxoglutarate as an acceptor of the amino group. The cellular concentration of 2-oxoglutarate in the *pycA* mutant, however, is very low, as indicated by the lack of ^{13}C incorporation into glutamate in the presence of [U-$^{13}C_6$]glucose. Aspartate oxidase, on the other hand, converts aspartate into oxaloacetate and ammonia in the presence of oxygen but generates hydrogen superoxide in the reaction, which might be too toxic for the listerial cell when produced in larger amounts. Thus, the generation of sufficient amounts of oxaloacetate from aspartate is apparently not possible in the *pycA* mutant.

Since even the addition of Casamino Acids, which provide all amino acids of the aspartate and glutamate families, cannot restore growth of the *pycA* mutant in the defined minimal medium, the shortage of oxaloacetate in the *pycA* mutant apparently leads to still other metabolic bottlenecks. One of them might be the insufficient production of other C_4 dicarboxylic acids, such as succinyl-CoA, which is needed for several metabolic reactions (19).

Metabolic adaptations of the mutant possibly encompass the lack of PYC when growing in BHI. The *pycA* mutant is able to grow (albeit more slowly than the wild-type strain) in BHI, a poorly defined rich culture medium. The transcript profiles of the two strains reveal significant changes in the metabolism of the *pycA* mutant compared to the wild-type strain. However, these data do not offer ready explanations for the ability of the mutant to grow in BHI but rather indicate that this ability is due to complex metabolic adaptation processes.

As shown in Table 1, the glucose metabolism in the *pycA* mutant is apparently reduced, as indicated by the downregulation of the glycolysis genes and the differential expression of many genes and operons that are activated or repressed by CcpA-dependent and -independent controls mediated by the cellular glucose concentrations in *B. subtilis* and *L. monocytogenes* (6, 16). This partial relief of these glucose-mediated gene control mechanisms could be a direct consequence of the *pycA* mutation, but the possibility that it is simply caused by the slower growth of the mutant in BHI cannot be excluded.

Upregulated genes and operons that seem to be differently controlled include the *fruRBA* operon (lmo2335 to lmo2337), the *pdu* genes (lmo1142 to lmo1150), and the *panBCD* genes (lmo1900 to lmo1902), as well as lmo0769 and lmo0865, encoding α-1,6-mannanase and phosphomannomutase (7). These genes are involved in glucose-independent carbon metabolism, and their upregulation suggests that the *pycA* mutant may utilize carbohydrates, such as fructose and/or mannose. These carbohydrates may derive from glycoproteins present in BHI.

The upregulation of the *panBCD* genes further suggests increased pantothenate production essential for the formation of coenzyme A. This cofactor is required for the synthesis of acetyl-CoA via oxidative decarboxylation of pyruvate by pyruvate dehydrogenase, a reaction that may be favored in the absence of PYC. An increased amount of acetyl-CoA may enhance the production of 2-oxoglutarate at low oxaloacetate concentrations, thereby stimulating the conversion of aspartate to oxaloacetate by aspartate aminotransferase (see above).

The upregulation of the genes encoding the enzymes for the complex, B_{12}-dependent propandiol utilization (Pdu) suggests that the *pycA* mutant possibly utilizes still other carbon substrates to overcome the lack of oxaloacetate production.

The impact of PYC on virulence. Our data show that the *pycA* mutant is taken up by macrophages at a rate similar to that of the wild-type strain. In contrast, the internalin-triggered internalization of the mutant by Caco-2 cells is about 100-fold lower than that of the wild-type strain. The internalization is carried out in RPMI medium, where the *pycA* mutant is unable to grow. The decreased internalization rate could therefore be due to altered surface structures of the *pycA* mutant. Alternatively, the internalin-triggered phagocytosis may require metabolically active listeriae, while the uptake by professional phagocytes may occur with metabolically inactive bacteria. In both host cell types, however, the *pycA* mutant is unable to replicate after being taken up, indicating that the intracellular milieu of the host cells—other than BHI—cannot compensate for the metabolic defect of the *pycA* mutation. As expected from the inability of the *pycA* mutant to replicate within mammalian cells, its virulence is also highly attenuated in the mouse sepsis model.

Due to the important role that PYC plays in the intracellular listerial metabolism and in systemic infections, the enzyme may represent an interesting metabolic target for the screening of antilisterial drugs.

ACKNOWLEDGMENTS

Victor Weidmann is acknowledged for performing mouse infection assays. We thank Sascha Stoll for helpful discussions and for critically reading the manuscript and Stephanie Grubmüller for help in the preparation of the manuscript.

This work was supported by the Deutsche Forschungsgemeinschaft (SFB479-B1, Go-168/27-3, and EI-384/6-1) and its priority program SPP1316 (EI-384/6 and FU-375/5), the Network of Excellence/EuroPathoGenomics, and the Fonds der chemischen Industrie.

REFERENCES

1. **Dussurget, O., J. Pizarro-Cerda, and P. Cossart.** 2004. Molecular determinants of *Listeria monocytogenes* virulence. Annu. Rev. Microbiol. **58:**587–610.
2. **Eisenreich, W., J. Slaghuis, R. Laupitz, J. Bussemer, J. Stritzker, C. Schwarz, R. Schwarz, T. Dandekar, W. Goebel, and A. Bacher.** 2006. ^{13}C isotopologue perturbation studies of *Listeria monocytogenes* carbon metabolism and its modulation by the virulence regulator PrfA. Proc. Natl. Acad. Sci. U. S. A. **103:**2040–2045.
3. **Eylert, E., J. Schär, S. Mertins, R. Stoll, A. Bacher, W. Goebel, and W. Eisenreich.** 2008. Carbon metabolism of *Listeria monocytogenes* growing inside macrophages. Mol. Microbiol. **69:**1008–1017.
4. **Freitag, N. E.** 2006. From hot dogs to host cells: how the bacterial pathogen *Listeria monocytogenes* regulates virulence gene expression. Future Microbiol. **1:**89–101.
5. **Fuchs, T. M., J. Klumpp, and K. Przybilla.** 2006. Insertion-duplication mutagenesis of *Salmonella enterica* and related species using a novel thermosensitive vector. Plasmid **55:**39–49.

6. **Fujita, Y.** 2009. Carbon catabolite control of the metabolic network in *Bacillus subtilis*. Biosci. Biotechnol. Biochem. **73:**245–259.
7. **Glaser, P., L. Frangeul, C. Buchrieser, C. Rusniok, A. Amend, F. Baquero, P. Berche, H. Bloecker, P. Brandt, T. Chakraborty, A. Charbit, F. Chetouani, E. Couvé, A. de Daruvar, P. Dehoux, E. Domann, G. Domínguez-Bernal, E. Duchaud, L. Durant, O. Dussurget, K. D. Entian, H. Fsihi, F. Garcia-del Portillo, P. Garrido, L. Gautier, W. Goebel, N. Gómez-López, T. Hain, J. Hauf, D. Jackson, L. M. Jones, U. Kaerst, J. Kreft, M. Kuhn, F. Kunst, G. Kurapkat, E. Madueno, A. Maitournam, J. M. Vicente, E. Ng, H. Nedjari, G. Nordsiek, S. Novella, B. de Pablos, J. C. Pérez-Diaz, R. Purcell, B. Remmel, M. Rose, T. Schlueter, N. Simoes, A. Tierrez, J. A. Vázquez-Boland, H. Voss, J. Wehland, and P. Cossart.** 2001. Comparative genomics of *Listeria* species. Science **294:**849–852.
8. **Hamon, M., H. Bierne, and P. Cossart.** 2006. *Listeria monocytogenes*: a multifaceted model. Nat. Rev. Microbiol. **4:**423–434.
9. **Janausch, I. G., E. Zientz, Q. H. Tran, A. Kroger, and G. Unden.** 2002. C4-dicarboxylate carriers and sensors in bacteria. Biochim. Biophys. Acta **1553:**39–56.
10. **Joseph, B., and W. Goebel.** 2007. Life of *Listeria monocytogenes* in the host cells' cytosol. Microbes Infect. **9:**1188–1195.
11. **Joseph, B., S. Mertins, R. Stoll, J. Schar, K. R. Umesha, Q. Luo, S. Muller-Altrock, and W. Goebel.** 2008. Glycerol-metabolism and PrfA activity in *Listeria monocytogenes*. J. Bacteriol. **190:**5412–5430.
12. **Joseph, B., K. Przybilla, C. Stühler, K. Schauer, J. Slaghuis, T. M. Fuchs, and W. Goebel.** 2006. Identification of *Listeria monocytogenes* genes contributing to intracellular replication by expression profiling and mutant screening. J. Bacteriol. **188:**556–568.
13. **Lecuit, M.** 2005. Understanding how *Listeria monocytogenes* targets and crosses host barriers. Clin. Microbiol. Infect. **11:**430–436.
14. **Marr, A. K., B. Joseph, S. Mertins, R. Ecke, S. Müller-Altrock, and W. Goebel.** 2006. Overexpression of PrfA leads to growth inhibition of *Listeria monocytogenes* in glucose-containing culture media by interfering with glucose uptake. J. Bacteriol. **188:**3887–3901.
15. **Mauder, N., R. Ecke, S. Mertins, D. I. Loeffler, G. Seidel, M. Sprehe, W. Hillen, W. Goebel, and S. Müller-Altrock.** 2006. Species-specific differences in the activity of PrfA, the key regulator of listerial virulence genes. J. Bacteriol. **188:**7941–7956.
16. **Mertins, S., B. Joseph, M. Goetz, R. Ecke, G. Seidel, M. Sprehe, W. Hillen, W. Goebel, and S. Müller-Altrock.** 2007. Interference of components of the phosphoenolpyruvate phosphotransferase system with the central virulence gene regulator PrfA of *Listeria monocytogenes*. J. Bacteriol. **189:**473–490.
17. **Premaratne, R. J., W. J. Lin, and E. A. Johnson.** 1991. Development of an improved chemically defined minimal medium for *Listeria monocytogenes*. Appl. Environ. Microbiol. **57:**3046–3048.
18. **Sambrook, J., and D. W. Russell.** 2001. Molecular cloning: a laboratory manual, 3rd ed. Cold Spring Harbor Laboratory Press, Cold Spring Harbor, NY.
19. **Sauer, U., and B. J. Eikmanns.** 2005. The PEP-pyruvate-oxaloacetate node as the switch point for carbon flux distribution in bacteria. FEMS Microbiol. Rev. **29:**765–794.
20. **Schnupf, P., and D. A. Portnoy.** 2007. Listeriolysin O: a phagosome-specific lysin. Microbes Infect. **9:**1176–1187.
21. **Scortti, M., H. J. Monzo, L. Lacharme-Lora, D. A. Lewis, and J. A. Vazquez-Boland.** 2007. The PrfA virulence regulon. Microbes Infect. **9:**1196–1207.
22. **Seveau, S., T. N. Tham, B. Payrastre, A. D. Hoppe, J. A. Swanson, and P. Cossart.** 2007. A FRET analysis to unravel the role of cholesterol in Rac1 and PI 3-kinase activation in the InlB/Met signalling pathway. Cell. Microbiol. **9:**790–803.

22a. **Stoll, R., and W. Goebel.** 7 January 2010. Identification of the major PEP-phosphotransferase systems (PTS) for glucose, mannose and cellobiose of Listeria monocytogenes and their significance for extra- and intracellular growth. Microbiology [Epub ahead of print.] doi:10.1099/mic.0.034934-0.

23. **Stülke, J., M. Arnaud, G. Rapoport, and I. Martin-Verstraete.** 1998. PRD-a protein domain involved in PTS-dependent induction and carbon catabolite repression of catabolic operons in bacteria. Mol. Microbiol. **28:**865–874.
24. **Tsai, H. N., and D. A. Hodgson.** 2003. Development of a synthetic minimal medium for *Listeria monocytogenes*. Appl. Environ. Microbiol. **69:**6943–6945.
25. **Warner, J. B., and J. S. Lolkema.** 2002. Growth of *Bacillus subtilis* on citrate and isocitrate is supported by the Mg^{2+}-citrate transporter CitM. Microbiology **148:**3405–3412.
26. **Wuenscher, M. D., S. Kohler, W. Goebel, and T. Chakraborty.** 1991. Gene disruption by plasmid integration in *Listeria monocytogenes*: insertional inactivation of the listeriolysin determinant *lisA*. Mol. Gen. Genet. **228:**177–182.
27. **Yang, Y. H., S. Dudoit, P. Luu, D. M. Lin, V. Peng, J. Ngai, and T. P. Speed.** 2002. Normalization for cDNA microarray data: a robust composite method addressing single and multiple slide systematic variation. Nucleic Acids Res. **30:**e15.
28. **Zamboni, N., H. Maaheimo, T. Szyperski, H. P. Hohmann, and U. Sauer.** 2004. The phosphoenolpyruvate carboxykinase also catalyzes C_3 carboxylation at the interface of glycolysis and the TCA cycle of *Bacillus subtilis*. Metab. Eng. **6:**277–284.